Surface-Induced Order Parameter Distortion in Superfluid ^{3}He-B Measured by Nonlinear NMR

Lev V. Levitin,[1,†] Robert G. Bennett,[1,2,*] Evgeny V. Surovtsev,[3] Jeevak M. Parpia,[2] Brian Cowan,[1] Andrew J. Casey,[1] and John Saunders[1]

[1]*Department of Physics, Royal Holloway University of London, Egham, TW20 0EX Surrey, United Kingdom*
[2]*Department of Physics, Cornell University, Ithaca, New York 14853, USA*
[3]*Kapitza Institute for Physical Problems, ul. Kosygina 2, Moscow 119334, Russia*

(Received 30 July 2013; published 6 December 2013)

The B phase of superfluid ^{3}He is a three-dimensional time-reversal invariant topological superfluid, predicted to support gapless Majorana surface states. We confine superfluid ^{3}He into a thin nanofluidic slab geometry. In the presence of a weak symmetry-breaking magnetic field, we have observed two possible states of the confined ^{3}He-B phase manifold, through the small tipping angle NMR response. Large tipping angle nonlinear NMR has allowed the identification of the order parameter of these states and enabled a measurement of the surface-induced gap distortion. The results for two different quasiparticle surface scattering boundary conditions are compared with the predictions of weak-coupling quasiclassical theory. We identify a textural domain wall between the two B phase states, the edge of which at the cavity surface is predicted to host gapless states, protected in the magnetic field.

DOI: 10.1103/PhysRevLett.111.235304 PACS numbers: 67.30.hr, 67.30.hj, 67.30.ht, 74.20.Rp

The concept of topological order in quantum condensed matter systems was first introduced to explain the quantum Hall effect [1] and to classify fractional quantum Hall states [2]. Following early work on superfluid ^{3}He [3] and with the recent prediction and discovery of the quantum spin Hall effect [4–6] and topological insulators [7–10], it has been extensively applied as a powerful tool in the classification of new states or phases of matter, complementing the established classification in terms of broken symmetries. See [11,12] for recent reviews. The construction of a periodic table for topological insulators and superconductors [13] has focused attention on topological superconductors, in part due to the prediction that these will host Majorana fermions. In particular, there is a search for odd-parity time-reversal invariant superconductors. The recent discovery of superconductivity in $Cu_xBi_2Se_3$, a copper intercalated topological insulator, has led to it being proposed as a candidate topological superconductor [14]. However, recent experimental evidence [15] points rather to this system being s-wave.

In this context there is naturally renewed interest in superfluid ^{3}He-B [16–18], as the established time-reversal invariant odd-parity condensate of p-wave pairs. The Bogoliubov–de Gennes Hamiltonian for ^{3}He-B, a fully gapped superfluid, corresponds to that of a 3D topological insulator [19]. The momentum space topology of ^{3}He-B was first extensively discussed by Volovik and co-workers [3,20]. The nontrivial topological invariant of this superfluid has Z_2 classification, as does the closely related planar state [16]. This bulk invariant necessarily gives rise, through bulk-boundary correspondence, to topologically protected gapless surface excitations.

The quasiclassical theory of superfluid ^{3}He provides the theoretical framework to calculate the influence of the surface in terms of the microscopic details of surface scattering of Bogoliubov quasiparticles [21]. It determines, self-consistently, the spatial dependence of the superfluid order parameter approaching the surface and the spectrum of the surface excitations (surface Andreev bound states). Conveniently for superfluid ^{3}He the surface scattering is subject to experimental control, via preplating with a superfluid ^{4}He film, and in principle by engineering the surface. For specular scattering these surface excitations are predicted to be Majorana fermions, with a linear dispersion relation [18].

Surface effects in superfluid ^{3}He can be studied at the free surface or at solid boundaries in bulk liquid, or in thin films. In previous experimental work, there is evidence of surface states with energy well below the bulk energy gap from the critical velocity of vibrating wires [22]; the contribution of surface bound states to the heat capacity has been detected in silver sinters [23], as well as contributions to the attenuation of transverse zero sound [24]. Furthermore, the spectrum of midgap surface excitations and its dependence on surface quasiparticle scattering has been investigated by measurements of the transverse acoustic impedance [25].

In this Letter we report an experimental study of the surface distortion of the ^{3}He-B order parameter within a single well-characterized nanofabricated slab geometry, of height $D = 0.7\ \mu$m approaching the superfluid coherence length $\xi_0 = \hbar v_F/2\pi k_B T_c$, where k_B is Boltzmann's constant, $\hbar$ is Planck's constant divided by 2π, v_F is the Fermi velocity, and T_c is the superfluid transition temperature. Using a sensitive SQUID NMR spectrometer, we measured the shifts of the precession relative to the Larmor frequency to probe the superfluid order parameter. We refer to [26] for a description of the new techniques we have developed for these measurements. In these nanofluidic

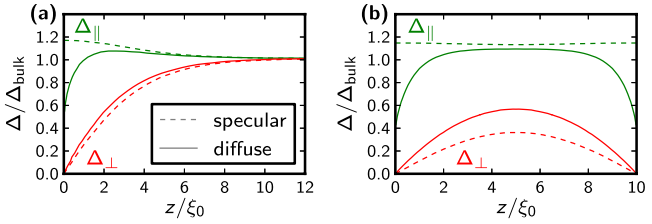

FIG. 1 (color online). Calculated spatial dependence of the two components of the B phase gap for diffuse (solid lines) and specular (dashed lines) boundaries (a) near a wall at $z = 0$ [41] and (b) in a slab of thickness $D = 10\xi_0$ [42].

samples the influence of the walls extends through the cavity. We show that the nonlinear response to pulsed NMR at large tipping angles allows us to conclusively identify the order parameter and characterize its surface-induced distortion.

Theoretically, the surface is predicted to induce a planar distortion of the B phase order parameter

$$\mathbf{\Delta}(\mathbf{p}) = \Delta_\parallel(z)(-\hat{p}_x + i\hat{p}_y)|\uparrow\uparrow\rangle + \Delta_\parallel(z)(\hat{p}_x + i\hat{p}_y)|\downarrow\downarrow\rangle + \Delta_\perp(z)\hat{p}_z[|\uparrow\downarrow\rangle + |\downarrow\uparrow\rangle], \quad (1)$$

where z is the direction of the surface normal. This expression describes states ranging from the bulk B phase with isotropic gap $\Delta_\perp = \Delta_\parallel$ to the planar phase where $\Delta_\perp = 0$, realized at the walls due to complete suppression of the pairs with orbital angular momentum in the plane of the walls. Typical profiles of $\Delta_\parallel(z)$ and $\Delta_\perp(z)$ are shown in Fig. 1. For p-wave pairing the order parameter can be represented as a matrix $\boldsymbol{A}$ via $\mathbf{\Delta}(\mathbf{p}) = i\boldsymbol{\sigma}_\mu\boldsymbol{\sigma}_y A_{\mu j}\hat{p}_j$, where $\boldsymbol{\sigma}_\mu$ are the Pauli matrices. The degenerate manifold of planar distorted B phase states is given by

$$A_{\mu j} = e^{i\phi}R_{\mu m}[\Delta_\parallel\delta_{mj} + (\Delta_\perp - \Delta_\parallel)\hat{o}_m\hat{o}_j], \quad (2)$$

where $\hat{\mathbf{o}}$ is the gap anisotropy axis, $e^{i\phi}$ is an overall phase factor, and the matrix $\boldsymbol{R} = \boldsymbol{R}(\hat{\mathbf{n}}, \theta)$ describes the rotation of spin relative to orbital coordinates by angle θ about axis $\hat{\mathbf{n}}$. In the state (1), $\theta = \phi = 0$. The degeneracy is lifted by the spin-orbit energy arising from the coherent nuclear dipole-dipole interaction and the nuclear Zeeman interaction in an applied magnetic field. The orientation of the order parameter ($\boldsymbol{R}$) is determined by the combined influence of these energies and the presence of surfaces [27,28].

Our experiment was performed in a static NMR field of 32 mT applied along the surface normal $\hat{\mathbf{z}}$ at a pressure of 5.5 bar. The B phase was observed below the transition from the A phase at $T_{AB} = 0.7T_c^{\rm bulk}$ [26], where $T_c^{\rm bulk} = 1.5$ mK is the bulk superfluid transition temperature. At this pressure $\xi_0 = 40$ nm. We first discuss our observations at the low temperature $T = 0.4T_c^{\rm bulk}$. The pulsed NMR signatures identified with the B phase are shown in Figs. 2(a) and 2(b). When probing with a small tipping angle, we sometimes observe a state B_+ with a positive

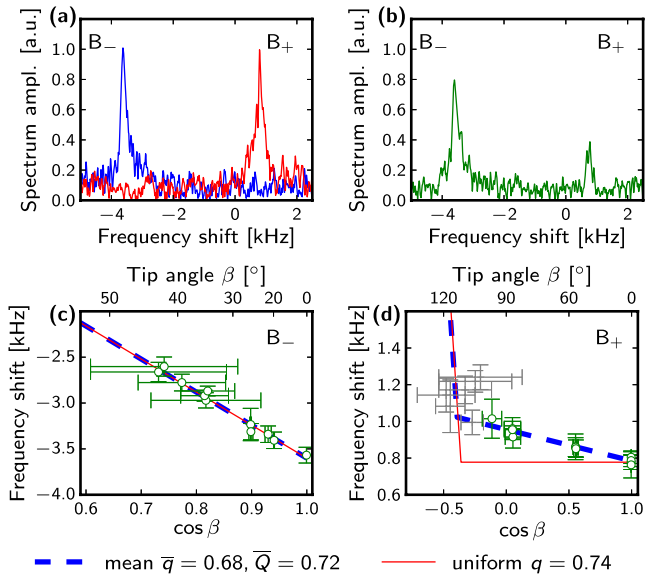

FIG. 2 (color online). NMR signatures of the B phase confined in the slab at $T = 0.4T_c^{\rm bulk}$. (a),(b) Spectra (Fourier transform of free-induction decay) observed after small tipping angle $\beta = 2°$ pulses on separate cooldowns from the A phase show either a positively shifted (B_+) or a negatively shifted (B_-) NMR line, or a combination [26]. (c),(d) Dependence of the frequency shift on the tipping angle β in nonlinear NMR experiments on B_- and B_+. These data provide a measurement of two gap distortion averages, $\bar{q}$ and $\bar{Q}$ (3). The B_+ data at $\beta < 104°$ only (green circles) were used in the fit, since magic angle $\beta^* > 104°$ for all $\bar{q}$ (see text). For comparison, the tipping angle dependence predicted for uniform planar distortion $q = \Delta_\perp/\Delta_\parallel$ is shown.

frequency shift relative to the normal state Larmor frequency, or a state B_- with a negative frequency shift, or a combination of both–different on each cooldown from the A phase [29]. This behavior is understood as follows.

The surface-induced planar distortion orients $\hat{\mathbf{o}} \parallel \hat{\mathbf{z}}$. The gap anisotropy gives rise to a magnetic susceptibility χ anisotropy with axis $\hat{\mathbf{w}} = \boldsymbol{R}\hat{\mathbf{o}}$. Since $\chi_\parallel > \chi_\perp$, in a field $\mathbf{H}$ the Zeeman energy, $F_H = -\frac{1}{2}\chi_\perp H^2 - \frac{1}{2}[\chi_\parallel - \chi_\perp]\times(\hat{\mathbf{w}}\cdot\mathbf{H})^2$, is minimized when $\hat{\mathbf{w}} = \pm\hat{\mathbf{H}}$. This anisotropy is much larger than the usual weak susceptibility anisotropy induced in the bulk B phase by a modest magnetic field, such as that used in our experiment, and is comparable to the strong anisotropy found in the A phase. In the static magnetic field of 32 mT the Zeeman interaction dominates over the dipole interaction and orients $\hat{\mathbf{w}}$. The two orientations $\hat{\mathbf{w}} = \hat{\mathbf{H}}$ and $\hat{\mathbf{w}} = -\hat{\mathbf{H}}$ have different dipole energies and give rise to the two distinct NMR responses [26,30].

The static magnetic field breaks the time-reversal invariance of the B phase. Along with a spin $\mathbf{S} = \boldsymbol{\chi}\mathbf{H}/\gamma$ (note that ^{3}He gyromagnetic ratio γ is negative) it induces, due to the superfluid order (2), a small orbital angular momentum $\mathbf{l} = -\boldsymbol{R}^{-1}\mathbf{S} = -\boldsymbol{R}^{-1}\boldsymbol{\chi}\mathbf{H}/\gamma$. The direction $\hat{\mathbf{l}}$ of this momentum can be used to classify the orientations. The B_+ state has $\hat{\mathbf{l}} = +\hat{\mathbf{H}}$, while $\hat{\mathbf{l}} = -\hat{\mathbf{H}}$ for B_- [30].

To establish the identification of B_+ and B_-, we performed NMR measurements of the superfluid frequency shift as a function of the tipping angle, shown in Figs. 2(c) and 2(d) [31]. We generalize the previous theory of the NMR in the B phase in the presence of a uniform planar distortion [32] to the present case where the planar distortion is spatially dependent. Our slab geometry imposes strong confinement on a length scale D much shorter than the dipole length $\xi_D \sim 10\ \mu$m set by the interplay of the dipole and gradient energies. Under such conditions the spin-orbit rotation $\boldsymbol{R}$ is uniform both in equilibrium and during the NMR precession; the equilibrium orientation and the spin dynamics are determined by the spatially averaged Zeeman and dipole energy.

The dipole energy is a sum of terms proportional to $\Delta_\parallel^2$, $\Delta_\parallel\Delta_\perp$, and $\Delta_\perp^2$, and we parametrize the relevant spatial averages as

$$\bar{q} = \frac{\langle \Delta_\parallel(z)\Delta_\perp(z)\rangle}{\langle \Delta_\parallel^2(z)\rangle}, \qquad \bar{Q} = \left[\frac{\langle \Delta_\perp^2(z)\rangle}{\langle \Delta_\parallel^2(z)\rangle}\right]^{1/2}. \tag{3}$$

For uniform planar distortion, $\bar{q} = \bar{Q} = \Delta_\perp/\Delta_\parallel$.

In the equilibrium state B_+ ($\hat{\mathbf{l}} = +\hat{\mathbf{H}}$) the spin-orbit rotation is about $\hat{\mathbf{n}} = \hat{\mathbf{z}}$ by $\theta = \arccos(-\bar{q}/4)$, and $\hat{\mathbf{w}} = \hat{\mathbf{o}} = \hat{\mathbf{n}}$. This orientation minimizes both the Zeeman and dipole energies and in the $\bar{q}$, $\bar{Q} \to 1$ limit corresponds to the orientation of the bulk B phase. The state B_- ($\hat{\mathbf{l}} = -\hat{\mathbf{H}}$), where $\hat{\mathbf{n}} \perp \hat{\mathbf{z}}$, $\theta = \pi$, and $\hat{\mathbf{w}} = -\hat{\mathbf{o}}$, does not minimize the dipole energy. This state is metastable in a magnetic field higher than the dipole field $H_D \sim 5$ mT, the field at which the Zeeman and dipole energies are comparable.

Importantly the nonlinear NMR response enables us to both confirm this state identification and determine the spatial averages $\bar{q}$, $\bar{Q}$ characterizing the order parameter distortion. We obtain the following frequency shift for $\hat{\mathbf{l}} = -\hat{\mathbf{H}}$:

$$\Delta f_-(\beta) = -\frac{\gamma^2\lambda_D N_F}{10\pi^2\langle\chi_\parallel\rangle f_L}\langle\Delta_\parallel^2\rangle[1 + 2\bar{Q}^2]\cos\beta. \tag{4}$$

In the prefactor in front of the squared gap N_F is the density of states, λ_D is the dipole energy strength constant [33], and $f_L = |\gamma H|/2\pi$ is the Larmor frequency. For $\hat{\mathbf{l}} = +\hat{\mathbf{H}}$,

$$\Delta f_+(\beta) = \frac{\gamma^2\lambda_D N_F}{10\pi^2\langle\chi_\parallel\rangle f_L}\langle\Delta_\parallel^2\rangle \times \begin{cases} 1 - \bar{q}^2 + 2(\bar{q}^2 - \bar{Q}^2)\cos\beta & \text{at } \cos\beta > \cos\beta^* \\ -1 - \bar{q} - 2(1 + 2\bar{q} + \bar{Q}^2)\cos\beta & \text{at } \cos\beta < \cos\beta^*. \end{cases} \tag{5}$$

Here, $\beta^* = \arccos(\bar{q} - 2)/(2\bar{q} + 2)$ is the magic angle which separates two modes of precession.

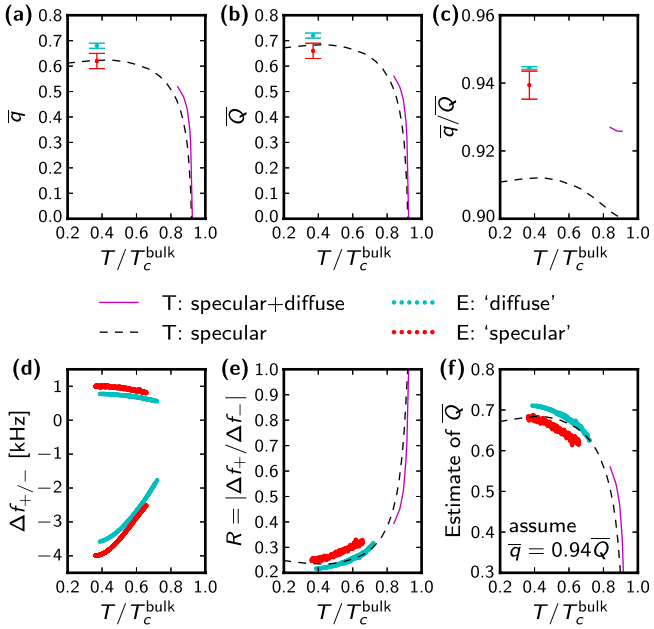

FIG. 3 (color online). Dependence of gap distortion on temperature and boundary conditions. (a),(b) Gap distortion predicted by quasiclassical theory [35], and results of nonlinear NMR; (c) predicted weak temperature dependence of ratio $\bar{q}/\bar{Q}$ of distortion parameters. (d) Temperature dependence of the small β frequency shifts Δf_+ and Δf_- in B_+ and B_- states; (e) their ratio; (f) inferred temperature dependence of average planar distortion assuming temperature-independent $\bar{q}/\bar{Q}$, in comparison with prediction [43]. The experimental data range is limited by the transition to the A phase [26].

It is apparent from Eq. (5) that the observed tip angle dependence of the frequency shift below the magic angle is a direct consequence of the nonuniformity of the planar distortion. Fits to the B_+ frequency shift below the magic angle, and the B_- data, Figs. 2(c) and 2(d), allow us to measure this distortion; we obtain $\bar{q} = 0.68$, $\bar{Q} = 0.72$ at this temperature [34].

We determine the temperature dependence of the average planar gap distortion from the ratio of the small tipping angle frequency shifts of the stable and metastable states $\Delta f_+(\beta \to 0)/|\Delta f_-(\beta \to 0)| = (1 + \bar{q}^2 - 2\bar{Q}^2)/(1 + 2\bar{Q}^2)$; see Fig. 3. The measurements were performed with two boundary conditions, "diffuse" and "specular," where the surface quasiparticle scattering is predominantly diffuse or specular, achieved by plating the cavity walls with ^{4}He [26]; the measurements as a function of the tipping angle discussed previously were with "diffuse" boundaries. We exploit the result of quasiclassical theory, Fig. 3(c), that $\bar{q}/\bar{Q}$ is only weakly temperature dependent [35]. We find reasonable agreement with the prediction of quasiclassical theory in the weak coupling limit, showing a smooth decrease of $\Delta_\perp$ as T_{AB} is approached. The dependence on quasiparticle surface scattering is in qualitative agreement with the theory: specular scattering enhances $\Delta_\parallel$ (see Fig. 1) and hence reduces $\bar{q}$ and $\bar{Q}$. In the weak

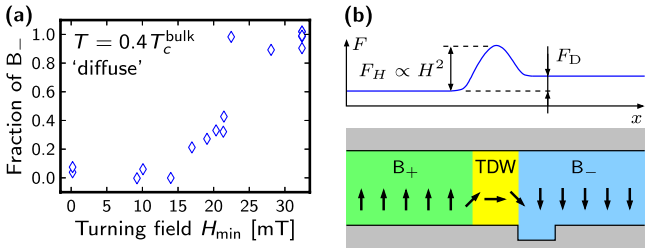

FIG. 4 (color online). Metastability of the B_- state. (a) By preparing the sample in B_- state, ramping the static field from 32 mT down to $H_{\rm min}$ and back (we can only interrogate the state of the sample in 32 mT), and measuring the relative weight of B_- and B_+ NMR signals, we probe the stability of B_- as a function of field $H_{\rm min}$. The $B_- \rightarrow B_+$ conversion is observed near $H^* = 20$ mT. (b) Textural domain wall (TDW) between B_+ and B_- and pinning mechanism. The arrows represent $\hat{\mathbf{l}}$, free-energy density F is shown schematically. The dipole energy F_D difference between B_- and B_+ pushes the wall to the right, expanding the B_+ domain; however, in a large enough field the domain wall is arrested ahead of a scratch on the cell surface by the Zeeman energy F_H of the domain wall.

coupling limit, the A phase is degenerate with the planar phase and $\Delta_\perp$ goes continuously to zero at T_{AB}. However, the strong coupling effects shift T_{AB} towards low temperatures [26], and $\Delta_\perp$ remains finite.

The observation of the coexistence of the two Ising-like states B_+ and B_-, Fig. 2(b), implies the existence of a domain wall [30]. The creation of the metastable B_- state and the stochastic nature of the coexistence of B_+ and B_- are consequences of the nucleation of the B phase at the first-order A-B transition. We attribute the stability of the coexistence of the higher energy B_- and lower energy B_+ domains to pinning of the domain walls at scratches on the cavity surface. Two classes of domain walls can exist in the B phase: those where the energy gap is distorted, termed "cosmological" [3], and textural, where only the orientation $\boldsymbol{R}$ changes [36,37]. The key difference between these is the domain wall energy cost, determined by pairing energy for the former, and Zeeman energy for the latter class. Consequently, the width of these domain walls is, respectively, of order ξ_0 and magnetic length $\xi_H = \xi_0[N_F\Delta_\parallel^2/(\chi_\parallel - \chi_\perp)H^2]^{1/2} \gg \xi_0$ [33], $\xi_H \sim 1\ \mu$m at 32 mT. Field cycling experiments allow us to identify the domain walls found here as textural. $B_- \rightarrow B_+$ conversion occurred when the static field was reduced, see Fig. 4(a), with an onset at $H^* \sim 20$ mT, significantly higher than the dipole field H_D. It can be explained by unpinning of textural domain walls at H^*, Fig. 4(b), and expansion of B_+ domains [38]. By contrast, the pinning of cosmological domain walls is field insensitive. Detecting the NMR signature of the domain walls is a goal of future work.

This domain wall, and the field-dependent pinning we observe, is of potential interest in the trapping and possible manipulation of Majorana fermions. The magnetic field breaks the time-reversal invariance required for the topological protection of surface zero modes, introducing a small gap $\sim\hbar\gamma H \ll \Delta$ in the dispersion relation [30,39]. However, inside the domain wall one-dimensional gapless states are predicted to be bound to the intersection of the domain wall with cavity surfaces [30]. Gapless surface states in the presence of a magnetic field have also been proposed for weak in-plane fields $H < H_D$ [39], in which case $\hat{l}_z = 0$, similar to the center of the textural domain wall, Fig. 4(b).

One of the motivations of this experiment was to search for the predicted "striped" or "crystalline superfluid" phase [40]. This state arises from the energetic stability of a domain wall between states of the B phase with opposite sign of $\Delta_\perp$ in (1). This is one of the cosmological domain walls classified in Ref. [3] predicted to host gapless bound states. The stripes are predicted to be as narrow as a few ξ_0 near the AB transition and grow wider on cooling. There is a large temperature range in which the width of the stripes W is smaller than ξ_D, where the spatial modulation of the order parameter along the cavity can be taken into account in the same way as the transverse gap inhomogeneity, leading to (4) and (5) with $\bar{q} = 0$, $\bar{Q} > 0$. Here, the weak additional components of the order parameter emerging at the domain walls [40] are neglected. Our measurements of $\bar{q}$, $\bar{Q} \neq 0$ at $T = 0.4T_c^{\rm bulk}$ rule out the striped phase with $W \ll \xi_D$ at this temperature, and the smooth temperature dependence of both $\Delta f_+(\beta \rightarrow 0)$ and $\Delta f_-(\beta \rightarrow 0)$ suggests that the B phase is stripe-free up to T_{AB}.

A conclusive experimental test for the stability of the striped phase requires more favorable experimental conditions than the present experiment: namely, an investigation of thicker slabs for which the B phase is stable at zero pressure, to minimize strong coupling effects, and with fully specular walls. This phase, if observed, would be a rare example of superfluid or superconducting order with spontaneously broken translational symmetry.

We thank G. Volovik for invaluable suggestions and both A. Vorontsov and J. Sauls for sharing calculations of the gap profile of ^{3}He in a planar geometry. This work was supported by EPSRC Grants No. EP/C522877/1, No. EP/E0541129/1, and No. EP/J022004/1, NSF Grant No. DMR-1202991, and the European Microkelvin Consortium (FP7 Grant No. 228464).

*Present address: Isentropic Ltd, 7, Brunel Way, Segensworth East, PO15 5TX, Hampshire, UK.
†l.v.Levitin@rhul.ac.uk

[1] D. J. Thouless, M. Kohmoto, M. P. Nightingale, and M. den Nijs, Phys. Rev. Lett. **49**, 405 (1982).
[2] X. G. Wen and A. Zee, Phys. Rev. B **46**, 2290 (1992).
[3] M. M. Salomaa and G. E. Volovik, Phys. Rev. B **37**, 9298 (1988).

[4] C. L. Kane and E. J. Mele, Phys. Rev. Lett. **95**, 146802 (2005).
[5] B. A. Bernevig, T. L. Hughes, and S. C. Zhang, Science **314**, 1757 (2006).
[6] M. König, S. Wiedmann, C. Brüne, A. Roth, H. Buhmann, L. W. Molenkamp, X.-Liang Qi, and S.-Cheng Zhang, Science **318**, 766 (2007).
[7] L. Fu, C. L. Kane, and E. J. Mele, Phys. Rev. Lett. **98**, 106803 (2007).
[8] J. E. Moore and L. Balents, Phys. Rev. B **75**, 121306 (2007).
[9] D. Hsieh, D. Qian, L. Wray, Y. Xia, Y. S. Hor, R. J. Cava, and M. Z. Hasan, Nature (London) **452**, 970 (2008).
[10] Y. Xia *et al.*, Nat. Phys. **5**, 398 (2009).
[11] M. Z. Hasan and C. L. Kane, Rev. Mod. Phys. **82**, 3045 (2010).
[12] X.-Liang Qi and S.-Cheng Zhang, Rev. Mod. Phys. **83**, 1057 (2011).
[13] A. P. Schnyder, S. Ryu, A. Furusaki, and A. W. W. Ludwig, Phys. Rev. B **78**, 195125 (2008).
[14] T. H. Hsieh and L. Fu, Phys. Rev. Lett. **108**, 107005 (2012)
[15] N. Levy, T. Zhang, J. Ha, F. Sharifi, A. A. Talin, Y. Kuk, and J. A. Stroscio, Phys. Rev. Lett. **110**, 117001 (2013).
[16] R. Roy, arXiv:0803.2868.
[17] X.-Liang Qi, T. L. Hughes, S. Raghu, and S.-Cheng Zhang, Phys. Rev. Lett. **102**, 187001 (2009).
[18] S. B. Chung and S.-Cheng Zhang, Phys. Rev. Lett. **103**, 235301 (2009).
[19] X.-Liang Qi, T. L. Hughes, and S.-Cheng Zhang, Phys. Rev. B **81**, 134508 (2010).
[20] G. E. Volovik, *The Universe in a Helium Droplet* (Oxford University Press, Oxford, England, 2003).
[21] J. W. Serene and D. Rainer, Phys. Rep. **101**, 221 (1983).
[22] C. A. M. Castelijns, K. F. Coates, A. M. Guénault, S. G. Mussett, and G. R. Pickett, Phys. Rev. Lett. **56**, 69 (1986).
[23] H. Choi, J. P. Davis, J. Pollanen, and W. P. Halperin, Phys. Rev. Lett. **96**, 125301 (2006).
[24] J. P. Davis, J. Pollanen, H. Choi, J. A. Sauls, W. P. Halperin, and A. B. Vorontsov, Phys. Rev. Lett. **101**, 085301 (2008).
[25] S. Murakawa, Y. Tamura, Y. Wada, M. Wasai, M. Saitoh, Y. Aoki, R. Nomura, Y. Okuda, Y. Nagato, M. Yamamoto, S. Higashitani, and K. Nagai, Phys. Rev. Lett. **103**, 155301 (2009).
[26] L. V. Levitin, R. G. Bennett, A. Casey, B. Cowan, J. Saunders, D. Drung, Th. Schurig, and J. M. Parpia, Science **340**, 841 (2013).
[27] H. Smith, W. F. Brinkman, and S. Engelsberg, Phys. Rev. B **15**, 199 (1977).
[28] A. I. Ahonen, M. Krusius, and M. A. Paalanen, J. Low Temp. Phys. **25**, 421 (1976).
[29] We observed B_+ alone on 57% of the cooldowns, B_- alone on 24%, and their combination on the remaining 19% (over the 37 cooldowns).
[30] G. E. Volovik, JETP Lett. **91**, 201 (2010).
[31] In these measurements, the evolution of the frequency of precession during free-induction decay after large pulses was observed and taken into account. Some uncertainty in tipping angle arose for large β, where we needed long pulses since the amplitude of NMR pulses we could use was limited by an associated heating, of unknown origin.
[32] Yu. M. Bunkov and G. E. Volovik, JETP **76**, 794 (1993).
[33] D. Vollhardt and P. Wölfle, *The superfluid phases of* ^{3}He (Taylor and Francis, London, 1990).
[34] We also obtain the gap suppression, although convoluted with the susceptibility, $\langle\Delta_\parallel^2\rangle/\langle\chi_\parallel\rangle = 0.49\Delta_B^2/\chi_B$, using an estimate of the bulk B phase Leggett frequency $\nu_B = [3\lambda_D N_F \Delta_B^2/4\pi^2\chi_B]^{1/2} = 170$ kHz.
[35] A. B. Vorontsov and J. A. Sauls, Phys. Rev. B **68**, 064508 (2003); (private communication).
[36] K. Maki and P. Kumar, Phys. Rev. B **16**, 4805 (1977).
[37] J. Kopu and M. Krusius, Phys. Rev. B **64**, 094504 (2001).
[38] This model relies on the assumption that there is always at least a small region of the sample in the B_+ state. The unpinning field H^* can be estimated by comparison of the energy gain of expanding B_+ to the cost of pushing the domain wall into a scratch. The observed field of 20 mT corresponds to a scratch $\delta D \sim D(H_D/H^*)^2 \sim 40$ nm deep, consistent with the depth of scratches observed by atomic force microscopy.
[39] T. Mizushima, M. Sato, and K. Machida, Phys. Rev. Lett. **109**, 165301 (2012).
[40] A. B. Vorontsov and J. A. Sauls, Phys. Rev. Lett. **98**, 045301 (2007); J. Low Temp. Phys. **138**, 283 (2005).
[41] Y. Nagato, M. Yamamoto, and K. Nagai, J. Low Temp. Phys. **110**, 1135 (1998).
[42] Y. Nagato and K. Nagai, Physica (Amsterdam) **284–288B**, 269 (2000).
[43] In our experiment, at the measuring pressure $D/\xi_0 = 18$. The calculations of [35] at a variety of D/ξ_0 were rescaled to this value; available calculations were for two specular walls and at $T > 0.84T_c^{\rm bulk}$ for one specular and one diffuse wall.